

# Layer potential identities and subtraction techniques

C. Carvalho

Applied Math Department, University of California Merced, USA

June 6, 2022

## Abstract

When using boundary integral equation methods, we represent solutions of a linear, partial differential equation as layer potentials. It is well-known that the approximation of layer potentials using quadrature rules suffer from poor resolution when evaluated closed to (but not on) the boundary. To address this challenge, we establish new layer potential identities that can be used to modify the solution's representation. Similar to Gauss's law used to modify Laplace's double-layer potential, we provide new identities to modify Laplace's single-layer potential and Helmholtz layer potentials that avoid the close evaluation problem. Several numerical examples illustrate the efficiency of the technique in two and three dimensions.

## 1 Introduction

One can represent the solution of partial differential boundary-value problems using boundary integral equation methods, which involves integral operators defined on the domain's boundary called layer potentials. Using layer potentials, the solution can be evaluated anywhere in the domain without restriction to a particular mesh. For that reason, boundary integral equations have found broad applications, including in fluid mechanics, electromagnetics, and plasmonics [40, 11, 31, 26, 3, 33, 32, 38].

The close evaluation problem refers to the nonuniform error produced by high-order quadrature rules used to discretize layer potentials. This phenomenon arises when computing the solution close to the boundary (i.e. at close evaluation points). It is well understood that this growth in error is due to the fact that the integrands of the layer potentials become increasingly peaked as the evaluation point approaches the boundary (nearly singular behavior), leading in limit cases to an  $O(1)$  error.

There exists a plethora of manners to address the close evaluation problem: using extraction methods based on a Taylor series expansions [39], regularizing the nearly singular behavior of the integrand and adding corrections [12, 13], compensating quadrature rules via interpolation [25], using Quadrature By Expansions related techniques (QBX) [10, 28, 21, 1, 37, 2, 41], using singularity subtraction techniques and interpolation [34, 36, 35], or using asymptotic approximations [18, 19, 27], to name a few. Most techniques rely on either providing corrections to the *kernel* (related to the fundamental

solution of the PDE at stake), or to the *density* (solution of the boundary integral equation).

In the latter category, it is well-known that Laplace's double-layer potential can be straightforwardly modified via a *density subtraction technique*, based on Gauss' law. This modification alleviates the close evaluation problem, and provides a better approximation for any given numerical method. However this technique is specific to Laplace's double-potential. In this paper we generalize Gauss' law by establishing new layer potential identities, for Laplace and Helmholtz. These identities involve both single- and double-potentials, and can be used to address the close evaluation problem in two and three dimensions. In particular, by modifying Laplace's single-potential (representing the solution of the exterior Neumann Laplace problem), a combination of Helmholtz double- and single-layer potentials (in the context of a sound-soft scattering problem), we obtain better approximations compared to standard representations, given some quadrature rule. The identities provide valuable insights into Laplace and Helmholtz layer potentials, and can also be applied to modify boundary integral equations to avoid weakly singular integrals.

The paper is organized as follows: section 2 presents known results and the considered boundary value problems, sections 3, 4 establish the layer potential identities and discuss their applications, sections 5, 6 illustrate the efficiency of the modified representations for Laplace and Helmholtz in two and three dimensions, off and on boundary. Finally, section 7 presents our concluding remarks, Appendices A, B provide a brief summary of the Nyström methods used in two and three dimensions, and Appendix C details some proofs for section 4.

## 2 Preliminaries and problems setting

### 2.1 The interior Dirichlet Laplace problem

Let us start by presenting known results. Consider a *domain*  $D \subset \mathbb{R}^d$ ,  $d = 2, 3$ , that is a bounded simply connected open set with smooth boundary (of class  $\mathcal{C}^2$ ). The interior Dirichlet problem for Laplace consists in finding  $u \in \mathcal{C}^2(D) \cap \mathcal{C}^1(\overline{D})$  such that

$$\begin{cases} \Delta u = 0 & D, \\ u = f & \partial D, \end{cases} \quad (1)$$

with some smooth data  $f$ . The solution of Problem (1) can be represented as a double-layer potential [23, 20]:

$$u(x) = \int_{\partial D} \partial_{n_y} G^L(x, y) \mu(y) d\sigma_y, \quad x \in D, \quad (2)$$

with  $n_y$  the unit outward normal of  $D$ ,  $G^L$  the fundamental solution of Laplace's equation

$$G^L(x, y) = \begin{cases} -\frac{1}{2\pi} \log |x - y| & \text{for } d = 2, \\ \frac{1}{4\pi} \frac{1}{|x - y|} & \text{for } d = 3, \end{cases} \quad (3)$$

$d\sigma_y$  is the integration surface element, and  $\mu$  a continuous density solution of the boundary integral equation:

$$-\frac{1}{2}\mu(x^*) + \int_{\partial D} \partial_{n_y} G^L(x^*, y) \mu(y) d\sigma_y = f(x^*), \quad x^* \in \partial D. \quad (4)$$

The fundamental solution  $G^L$  is singular when  $y = x^*$ , and *nearly singular* when  $|x - y| \rightarrow 0$  for  $x \in D$ . The layer potential is said to be a weakly singular integral (resp. a nearly singular integral) when its kernel (given here by  $\partial_{n_y} G^L(x, \cdot)$ ) is singular (resp. nearly singular). There exist high-order quadrature rules to approximate weakly singular integrals with very high accuracy (e.g. [9, 15, 22, 14]). However, high accuracy is lost for nearly singular integrals: this is the so-called close evaluation problem. There exists a well-known straightforward modification of (2) that alleviates this problem, for any chosen approximation method. Using Gauss's law [23]

$$\int_{\partial D} \partial_{n_y} G^L(x, y) d\sigma_y = \begin{cases} -1 & x \in D, \\ -\frac{1}{2} & x \in \partial D, \\ 0 & x \in \mathbb{R}^d \setminus \bar{D}, \end{cases} \quad (5)$$

and assuming we can write any  $x \in D$  as  $x = x^* - \ell n_{x^*}$ , with  $x^* \in \partial D$ ,  $n_{x^*}$  the unit outward normal at  $x^*$ , and  $\ell > 0$  the distance from the boundary (see Figure 1), then one can write (2) as

$$u(x) = \int_{\partial D} \partial_{n_y} G^L(x, y) [\mu(y) - \mu(x^*)] d\sigma_y - \mu(x^*). \quad (6)$$

The integrand in (6) now vanishes at  $y = x^*$ , which corresponds to the point where the

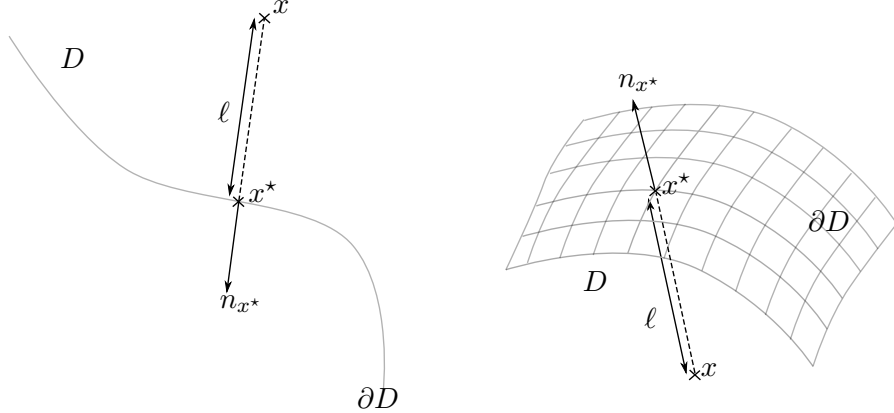


Figure 1 – Sketch of the quantities introduced to study evaluation points close to the boundary in 2D (left) and in 3D (right).

kernel is nearly singular. Representation (6) presents advantages as there is no nearly singular behavior to approximate anymore. This modified representation is specific to the double-layer potential, and cannot be used for the single-layer potential, or other boundary value problems.

## 2.2 The exterior Neumann Laplace problem

Using previous notations, the exterior Neumann problem for Laplace consists in finding  $u \in \mathcal{C}^2(E) \cap \mathcal{C}^1(\bar{E})^1$ , with  $E := \mathbb{R}^d \setminus \bar{D}$ , such that

$$\begin{cases} \Delta u = 0 & E, \\ \partial_{n_y} u = g & \partial D, \end{cases} \quad (7)$$

with some smooth data  $g$ . The solution of Problem (7) can be represented as a single-layer potential [23, 20]:

$$u(x) = \int_{\partial D} G^L(x, y) \rho(y) d\sigma_y, \quad x \in D, \quad (8)$$

with  $\rho$  a continuous density solution of the boundary integral equation:

$$\frac{1}{2} \rho(x^*) + \int_{\partial D} \partial_{n_x} G^L(x^*, y) \rho(y) d\sigma_y = g(x^*), \quad x^* \in \partial D. \quad (9)$$

The representation (8) suffers as well from the close evaluation problem, and contrary to problem (1), there are no subtraction techniques (based on identities such as Gauss' law) available to address the problem.

## 2.3 Sound-soft acoustic scattering problem

The sound-soft scattering problem consists in finding  $u \in \mathcal{C}^2(E) \cup \mathcal{C}^1(\bar{E})$  such that

$$\begin{cases} \Delta u + k^2 u = 0 & E, \\ u = f & \partial D, \\ \lim_{R \rightarrow \infty} \int_{|y|=R} \partial_{n_y} u - iku d\sigma_y = 0, \end{cases} \quad (10)$$

with some smooth data  $f$  associated to the wavenumber  $k$ . Above, the last condition represents the Sommerfeld radiation condition. The solution of Problem (10) can be represented as a combination of double- and single-layer potentials [30]:

$$u(x) = \int_{\partial D} [\partial_{n_y} G^H(x, y) - ikG^H(x, y)] \mu(y) d\sigma_y, \quad x \in E, \quad (11)$$

with  $G^H$  defined by

$$G^H(x, y) = \begin{cases} \frac{i}{4} H_0^{(1)}(k|x - y|), & \text{for } d = 2, \\ \frac{1}{4\pi} \frac{e^{ik|x-y|}}{|x - y|}, & \text{for } d = 3, \end{cases} \quad (12)$$

---

1. We denote  $\bar{E} := \mathbb{R}^d \setminus D$ .

with  $H_0^{(1)}(\cdot)$  the Hankel function of first kind, and  $\mu$  a continuous density satisfying:

$$\frac{1}{2}\mu(x^*) + \int_{\partial D} [\partial_{n_y} G^H(x^*, y) - ikG^H(x^*, y)] \mu(y) d\sigma_y = f(x^*), \quad x^* \in \partial D. \quad (13)$$

As previously, representation (11) suffers from the close evaluation problem, and there are no subtraction techniques (based on identities such as Gauss' law) available to address the problem.

**Remark 1.** *There already exists efficient techniques to address the close evaluation problem, such as using regularized kernels for Laplace [12, 13], or density plane-wave expansions for wave problems [34, 36]. In this paper we derive general layer potential identities that provide valuable insight into Laplace's and Helmholtz layer potentials, and can be also used to address the close evaluation problem.*

### 3 Layer potentials identities

From now on we denote  $u_{\text{sol}}^L$  a solution of Laplace's equation in  $D \subset \mathbb{R}^d$ ,  $u_{\text{sol}}^H$  a solution of Helmholtz equation in  $D$ , respectively.

**Theorem 1** (Layer potential identity). *Given  $G^e$ ,  $e = L, H$ , for any  $u_{\text{sol}}^e$ ,  $e = L, H$  we have:*

$$\int_{\partial D} \partial_{n_y} G^e(x, y) u_{\text{sol}}^e(y) - G^e(x, y) \partial_{n_y} u_{\text{sol}}^e(y) d\sigma_y = \begin{cases} -u_{\text{sol}}^e(x) & x \in D \\ -\frac{1}{2}u_{\text{sol}}^e(x) & x \in \partial D \\ 0 & x \in E \end{cases} \quad (14)$$

Note that the results for  $x \in D$ , and  $x \in E$  are well-known, and come from the representation formula (e.g. [29, Theorem 6.5], [20, Theorem 3.1]). What is new is the result on the boundary, and the proof follows the same steps as the proof of Gauss' law [23, 16, 20].

*Proof.* Given  $x \in \mathbb{R}^d$ ,  $d = 2, 3$ , we define  $\Omega_{x, \varepsilon}$  the ball of center  $x$  and radius  $\varepsilon$ . Consider  $x^* \in \partial D$  and define  $H_{x^*, \varepsilon}$  the part of  $\partial\Omega_{x^*, \varepsilon}$  that is contained in  $D$ . Define also  $D_\varepsilon := D \setminus \overline{\Omega_{x^*, \varepsilon}}$ . Using Green's second identity, we find that:

$$\int_{\partial D_\varepsilon} \partial_{n_y} G^e(x^*, y) u_{\text{sol}}^e(y) - G^e(x^*, y) \partial_{n_y} u_{\text{sol}}^e(y) d\sigma_y = 0, \quad e = L, H.$$

Noting that  $\partial D_\varepsilon = H_{x^*, \varepsilon} \cup (\partial D \setminus H_{x^*, \varepsilon})$ , then we have

$$\int_{\partial D} \partial_{n_y} G^e(x^*, y) u_{\text{sol}}^e(y) - G^e(x^*, y) \partial_{n_y} u_{\text{sol}}^e(y) d\sigma_y = -\lim_{\varepsilon \rightarrow 0} I_\varepsilon^e, \quad e = L, H,$$

with  $I_\varepsilon^e := \int_{H_{x^*, \varepsilon}} \partial_{n_y} G^e(x^*, y) u_{\text{sol}}^e(y) - G^e(x^*, y) \partial_{n_y} u_{\text{sol}}^e(y) d\sigma_y$ ,  $e = L, H$ . One just needs to compute the right-hand side to conclude. Because we make use of parameterization

explicitly, we treat the two dimensional case and the three dimensional case separately.

**In two dimensions:**  $H_{x^*, \varepsilon}$  can be parameterized by  $y(t) = x^* + (\varepsilon \cos t, \varepsilon \sin t)$ ,  $t \in [0, \pi]$ . Using the regularity of the solution  $u_{\text{sol}}^e$ ,  $e = L, H$ , we obtain

$$\begin{aligned} I_\varepsilon^L &= \int_0^\pi \left( \frac{1}{2\pi\varepsilon} (u_{\text{sol}}^L(x^*) + O(\varepsilon)) + \frac{1}{2\pi} \log(\varepsilon) (\partial_{n_y} u_{\text{sol}}^L(x^*) + O(\varepsilon)) \right) \varepsilon dt \\ &= \frac{u_{\text{sol}}^L(x^*)}{2} + O(\varepsilon \log(\varepsilon)). \end{aligned}$$

Taking the limit as  $\varepsilon \rightarrow 0$  finishes the proof. One obtains the same results for  $I_\varepsilon^H$ , using the results [16]:  $G^H(x^*, y(t)) = G^L(x^*, y(t)) + O(\varepsilon \log(\varepsilon))$ ,  $\partial_{n_y} G^H(x^*, y(t)) = \partial_{n_y} G^L(x^*, y(t)) + O(1)$ .

**In three dimensions:**  $H_{x^*, \varepsilon}$  can be parameterized by

$y(s, t) = x^* + (\varepsilon \sin s \cos t, \varepsilon \sin s \sin t, \varepsilon \cos s)$ ,  $s \in [0, \frac{\pi}{2}]$ ,  $t \in [-\pi, \pi]$ . Then we have

$$\begin{aligned} I_\varepsilon^L &= \frac{1}{4\pi} \int_{-\pi}^\pi \int_0^{\pi/2} \left( \frac{1}{\varepsilon^2} (u_{\text{sol}}^L(x^*) + O(\varepsilon)) - \frac{1}{\varepsilon} (\partial_{n_y} u_{\text{sol}}^L(x^*) + O(\varepsilon)) \right) \varepsilon^2 \sin(s) ds dt \\ &= \frac{1}{4\pi} \int_{-\pi}^\pi \int_0^{\pi/2} (u_{\text{sol}}^L(x^*) + O(\varepsilon)) \sin(s) ds dt, \\ &= \frac{u_{\text{sol}}^L(x^*)}{2} + O(\varepsilon), \\ I_\varepsilon^H &= \frac{1}{4\pi} \int_{-\pi}^\pi \int_0^{\pi/2} \left( \frac{1}{\varepsilon} - ik \right) \frac{e^{ik\varepsilon}}{\varepsilon} (u_{\text{sol}}^H(x^*) + O(\varepsilon)) \varepsilon^2 \sin(s) ds dt \\ &\quad - \frac{1}{4\pi} \int_{-\pi}^\pi \int_0^{\pi/2} \frac{e^{ik\varepsilon}}{\varepsilon} (\partial_{n_y} u_{\text{sol}}^H(x^*) + O(\varepsilon)) \varepsilon^2 \sin(s) ds dt, \\ &= \frac{1}{4\pi} \int_{-\pi}^\pi \int_0^{\pi/2} (u_{\text{sol}}^H(x^*) + O(\varepsilon)) e^{ik\varepsilon} \sin(s) ds dt, \\ &= \frac{u_{\text{sol}}^H(x^*)}{2} e^{ik\varepsilon} + O(\varepsilon). \end{aligned}$$

Taking the limit as  $\varepsilon \rightarrow 0$  finishes the proof.  $\square$

## 4 Consequences from Theorem 1

Naturally, we recover Gauss' law using  $u_{\text{sol}}^L \equiv 1$  in (14). Nonetheless one can establish new identities involving both double-and single-layer potentials. We present some examples below.

## 4.1 New identities

We consider a linear function  $u_{\text{sol}}^L \equiv a \cdot x$ , with  $a \in \mathbb{R}^d$ , and  $u_{\text{sol}}^L \equiv G^L(x, x_0)$  with  $x_0 \in E$ . Both satisfy Laplace's equation in  $D$  and Theorem 1 gives us

$$\int_{\partial D} \partial_{n_y} G^L(x, y) (n_y \cdot a) - G^L(x, y) (a \cdot y) d\sigma_y = \begin{cases} -a \cdot x & x \in D \\ -\frac{1}{2} a \cdot x & x \in \partial D \\ 0 & x \in E \end{cases}$$

and

$$\int_{\partial D} \partial_{n_y} G^L(x, y) G^L(y, x_0) - G^L(x, y) \partial_{n_y} G^L(y, x_0) d\sigma_y = \begin{cases} -G^L(x, x_0) & x \in D \\ -\frac{1}{2} G^L(x, x_0) & x \in \partial D \\ 0 & x \in E \end{cases}$$

Those identities could be used to modify (2), and especially (8), to address the close evaluation problem. Note that chosen  $u_{\text{sol}}^L$  are not solutions of problem (7). We discuss their applications in sections 4.2-4.3.

Now consider a plane wave  $u_{\text{sol}}^H \equiv e^{iks \cdot x}$ , with  $s \in \mathbb{S}^{d-1}$ , and  $u_{\text{sol}}^H \equiv G^H(x, x_0)$  with  $x_0 \in E$ . Both satisfy Helmholtz equation in  $D$  and Theorem 1 gives us

$$\int_{\partial D} (\partial_{n_y} G^H(x, y) - ik(n_y \cdot s) G^H(x, y)) e^{iks \cdot y} d\sigma_y = \begin{cases} -e^{iks \cdot x} & x \in D \\ -\frac{1}{2} e^{iks \cdot x} & x \in \partial D \\ 0 & x \in E \end{cases}$$

and

$$\int_{\partial D} \partial_{n_y} G^H(x, y) G^H(y, x_0) - G^H(x, y) \partial_{n_y} G^H(y, x_0) d\sigma_y = \begin{cases} -G^H(x, x_0) & x \in D \\ -\frac{1}{2} G^H(x, x_0) & x \in \partial D \\ 0 & x \in E \end{cases}$$

Note that chosen  $u_{\text{sol}}^H$  are not solutions of Problem (10). Again, those identities could be used to modify (11) to address the close evaluation problem, which is discussed in section 4.4.

## 4.2 Modified Laplace double-layer potential

Let  $u_{\text{sol}}^L$  be a solution of Laplace's equation in  $D \subset \mathbb{R}^d$ ,  $d = 2, 3$ . Writing  $x \in D$  as  $x = x^* - \ell n_{x^*}$ , with  $x^* \in \partial D$ , one can show that the solution of the interior Dirichlet

Laplace problem (1) admits the modified representation:

$$\begin{aligned}
u(x) = & \int_{\partial D} \partial_{n_y} G^L(x, y) \mu(y) [1 - u_{\text{sol}}^L(y)] d\sigma_y + \int_{\partial D} \partial_{n_y} G^L(x, y) [\mu(y) - \mu(x^*)] u_{\text{sol}}^L(y) d\sigma_y \\
& - \mu(x^*) u_{\text{sol}}^L(x^*) + \mu(x^*) \int_{\partial D} G^L(x, y) \mu(y) [\partial_{n_y} u_{\text{sol}}^L(y) - \partial_{n_y} u_{\text{sol}}^L(x^*)] d\sigma_y \\
& + \mu(x^*) \partial_{n_y} u_{\text{sol}}^L(x^*) \int_{\partial D} G^L(x, y) \mu(y) d\sigma_y,
\end{aligned} \tag{15}$$

(see Appendix C.1). The modified representation (15) addresses the close evaluation problem, in the sense that nearly singular terms vanish at  $y = x^*$ , as long as

$$u_{\text{sol}}^L(x^*) = 1, \quad \partial_{n_y} u_{\text{sol}}^L(x^*) = 0. \tag{16}$$

Typically, solutions of Laplace's equation in  $D$  are either constant, linear, or of the form  $G^L(x, x_0)$  with  $x_0 \in E$ . The only one that satisfies the conditions (16) is  $u_{\text{sol}}^L \equiv 1$ , then the modified representation (15) boils down to (6). As a consequence the modified representation (6) is the only one with practicability.

### 4.3 Modified Laplace single-layer potential

One can show the following (see Appendix C.2 for details)

**Proposition 1.** *Given  $x = x^* + \ell n_{x^*} \in E$  with  $x^* \in \partial D$ , let  $u_{\text{sol}}^L$  be a solution of Laplace's equation in  $D \subset \mathbb{R}^d$ ,  $d = 2, 3$ , such that*

$$\partial_{n_y} u_{\text{sol}}^L(x^*) = 1. \tag{17}$$

*The solution of the exterior Neumann Laplace problem (7) admits the modified representation:*

$$\begin{aligned}
u(x) = & \int_{\partial D} G^L(x, y) \mu(y) [1 - \partial_{n_y} u_{\text{sol}}^L(y)] d\sigma_y \\
& + \int_{\partial D} G^L(x, y) [\mu(y) - \mu(x^*)] \partial_{n_y} u_{\text{sol}}^L(y) d\sigma_y \\
& + \mu(x^*) \int_{\partial D} \partial_{n_y} G^L(x, y) \mu(y) [u_{\text{sol}}^L(y) - u_{\text{sol}}^L(x^*)] d\sigma_y.
\end{aligned} \tag{18}$$

*The modified representation (18) has no nearly singular integrals.*

In this case, constant solutions like  $u_{\text{sol}}^L \equiv 1$  do not satisfy (17), however one can check that

- the linear function  $u_{\text{sol}}^L(y) = n_{x^*} \cdot y$  ;
- the Green-based function  $u_{\text{sol}}^L(y) = 2^{d-1} \pi G^L(y, x^* + n_{x^*})$  ;

do satisfy (17). In section 5 we will test (18) using both linear and Green-based  $u_{\text{sol}}^L$ . The modified representation (18) adds two terms to compute compared to (8), it is the price to pay to gain accuracy at close evaluation points.

#### 4.4 Modified Helmholtz layer potentials

**Proposition 2.** *Given  $x = x^* + \ell n_{x^*} \in E$  with  $x^* \in \partial D$ , let  $u_{sol}^H$  be a solution of Helmholtz equation in  $D \subset \mathbb{R}^d$ ,  $d = 2, 3$ , such that*

$$u_{sol}^H(x^*) = 1, \quad \partial_{n_y} u_{sol}^H(x^*) = ik. \quad (19)$$

*Then the solution of the sound-soft scattering problem (10) admits the modified representation:*

$$\begin{aligned} u(x) = & \int_{\partial D} [\partial_{n_y} G^H(x, y) - \partial_{n_y} u_{sol}^H(y) G^H(x, y)] [\mu(y) - \mu(x^*)] d\sigma_y \\ & + \int_{\partial D} G^H(x, y) [\partial_{n_y} u_{sol}^H(y) - ik] \mu(y) d\sigma_y \\ & + \mu(x^*) \int_{\partial D} \partial_{n_y} G^H(x, y) [1 - u_{sol}^H(y)] d\sigma_y. \end{aligned} \quad (20)$$

*The modified representation (20) has no nearly singular integrals.*

The proof can be found in Appendix C.3. One can check that plane waves  $u_{sol}^H(y) = e^{ikn_{x^*} \cdot (y - x^*)}$  do satisfy (19), whereas Green-based functions like  $u_{sol}^H(y) = G^H(y, x_* + n_{x^*})$  (up to some constant) cannot. We will use (20) with plane waves for the numerical examples.

### 5 Numerical examples

The accuracy in approximating (2)-(6), (8)-(18), (11)-(20) respectively, relies on the resolution of the boundary integral equation (4), (9), (13) respectively. In what follows we assume that the boundary integral equations are sufficiently resolved, and given the density's resolution, we compare the representations and their modified ones through several examples. All the codes can be found in [17].

#### 5.1 Exterior Neumann Laplace problem

Using Proposition 1, we compare (8) with the modified representation (18) obtained with  $u_{sol}^L(y) = n_{x^*} \cdot y$ , and with  $u_{sol}^L(y) = 2^{d-1}\pi G^L(y, x^* + n^*)$ : for any  $x \in E$

$$\begin{aligned} u(x) = & \int_{\partial D} G^L(x, y) \mu(y) [1 - n_y \cdot n_{x^*}] d\sigma_y \\ & + \int_{\partial D} G^L(x, y) [\mu(y) - \mu(x^*)] n_y \cdot n_{x^*} d\sigma_y \\ & + \mu(x^*) \int_{\partial D} \partial_{n_y} G^L(x, y) \mu(y) n_{x^*} \cdot (y - x^*) d\sigma_y, \end{aligned} \quad (21)$$

$$\begin{aligned}
u(x) = & \int_{\partial D} G^L(x, y) \mu(y) \left[ 1 + \frac{n_y \cdot (y - x^* - n_{x^*})}{|y - x^* - n_{x^*}|^d} \right] d\sigma_y \\
& - \int_{\partial D} G^L(x, y) [\mu(y) - \mu(x^*)] \frac{n_y \cdot (y - x^* - n_{x^*})}{|y - x^* - n_{x^*}|^d} d\sigma_y \\
& + \mu(x^*) 2^{d-1} \pi \int_{\partial D} \partial_{n_y} G^L(x, y) \mu(y) [G^L(y, x^* + n_{x^*}) - G^L(x^*, x^* + n_{x^*})] d\sigma_y.
\end{aligned} \tag{22}$$

We'll refer to (21) as the modified representation using *Density Subtraction with Linear solution* technique (DSL), (22) as the modified representation using *Density Subtraction with Green-based solution* technique (DSG), respectively.

### 5.1.1 Example 1: exterior Laplace in two dimensions

Since  $\partial D$  is a closed smooth boundary, we use the Periodic Trapezoid Rule (PTR) to approximate (8)-(21)-(22).

We consider an exact solution of Problem (7):

$$u_{\text{exact}}(x) = u_{\text{exact}}(x_1, x_2) = \frac{x_1 - x_{0,1}}{|x - x_0|^2}, \quad x_0 = (x_{0,1}, x_{0,2}) \in D,$$

which consists in choosing  $g(x^*) = \partial_{n_y} u_{\text{exact}}(x^*)$ , for any  $x^* \in \partial D$ . Figures 2-3 represent the error obtained on a kite-shaped domain using:

- **PTR:** approximation of (8) using the Periodic Trapezoid Rule.
- **DSL:** approximation of (21) using the Periodic Trapezoid Rule.
- **DSG:** approximation of (22) using the Periodic Trapezoid Rule.

For all simulations we consider  $N = 128$  quadrature points.

We solved (9) using Periodic Trapezoid Rule. The accuracy of all methods is limited by the accuracy of the resolution for  $\mu$ . Results in Figures-2-3 show that, given  $\mu$  resolved, the approximation of the modified representations provide better results overall. Far from the boundary, all methods approximate well the solution. As the evaluation point gets closer to the boundary ( $\ell \rightarrow 0$ ), PTR suffers from the close evaluation problem and the error increases. Note that the single-layer potential commonly suffers less from this phenomenon than the double-layer potential (e.g. [18]). Using the modified representations (DSL-DSG) allows to reduce the error by a couple of order of magnitude for the close evaluation problem. Both modified representations provide a satisfactory corrections overall. Using a naïve (straightforward) implementation of (8)-(21)-(22), PTR is obviously cheaper (less terms to compute) than DSL and DSG, and DSL is cheaper than DSG due to simpler terms (and less operations to conduct). Therefore DSL seems the best choice for the best computational cost-accuracy trade-off. In the next section we investigate the efficacy of DSL in three dimensions.

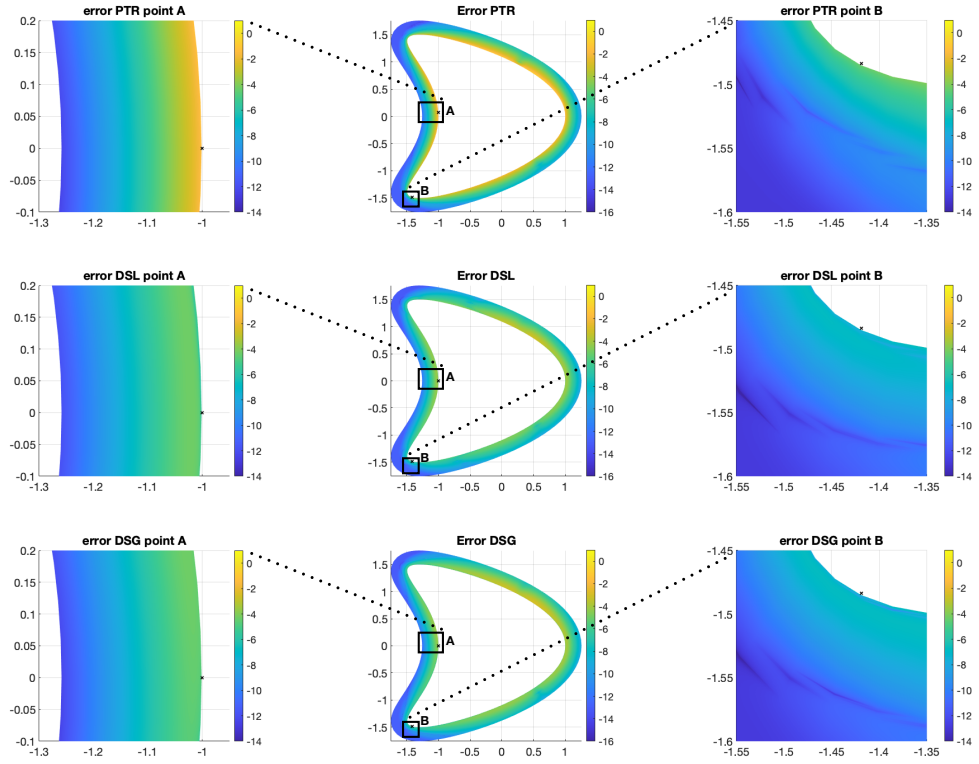


Figure 2 – Plots of  $\log_{10}$  of the error for the evaluation of the solution of (7) out of the kite domain defined by the boundary  $y(t) = (\cos t + 0.65 \cos(2t) - 0.65, 1.5 \sin t)$ ,  $t \in [0, 2\pi]$ , for the Neumann data,  $g(x^*) = \partial_{n_y} u_{\text{exact}}(x^*)$  with  $x_0 = (0.1, 0.4)$ , using PTR (top), DSL (middle), DSG (bottom), with  $N = 128$ . Obtained run times: 0.375721s for PTR, 0.416045s for DSL, 0.638421s for DSG.

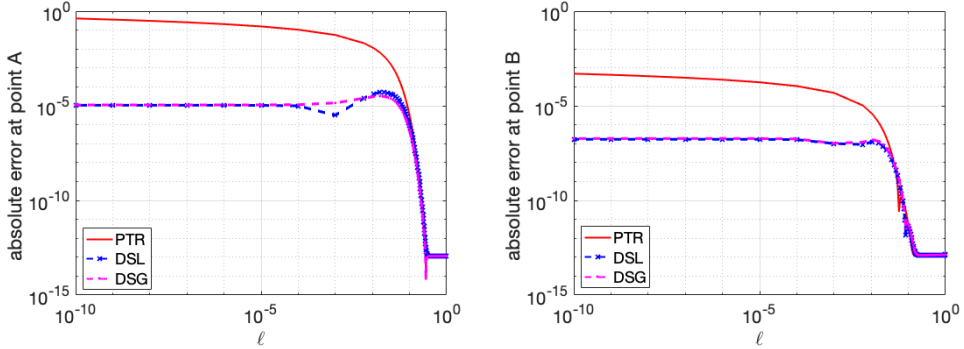


Figure 3 – Log-log plots of the errors made in computing the solution along the normal of the two points A, B, plotted as black  $\times$ 's in Figure 2.

### 5.1.2 Example 2: exterior Laplace in three dimensions

We assume  $\partial D$  to be an analytic, closed, and oriented surface that can be parameterized by  $y = y(s, t)$  for  $s \in [0, \pi]$  and  $t \in [-\pi, \pi]$ . Then one can write (8) as

$$u(x) = \int_{-\pi}^{\pi} \int_0^{\pi} G(x, y(s, t)) J(s, t) \rho(y(s, t)) \sin(s) ds dt, \quad (23)$$

with  $J(s, t) = |y_s(s, t) \times y_t(s, t)|/\sin(s)$  the Jacobian. We now work with a surface integral defined on a sphere, and we use a three-step method (see [27] for details) to approximate (8)-(21). This method has been shown to be effective for computing layer potentials in three dimensions, in particular for close evaluations. It relies on (i) rotating the local coordinate system so that  $x^*$  corresponds to the north pole, (ii) use Periodic Trapezoid Rule with  $2N$  quadrature points to approximate the integral with respect to  $t$ , (iii) use Gauss-Legendre with  $N$  quadrature points mapped to  $(0, \pi)$  (and not  $(-1, 1)$ ) to approximate the integral with respect to  $s$ . This leads to the approximation:

$$u(x) \approx \frac{\pi^2}{2N} \sum_{i=1}^N \sum_{j=1}^{2N} w_i \sin(s_i) F(s_i, t_j),$$

with  $F(s_i, t_j) = G(x, y(s_i, t_j)) J(s_i, t_j) \rho(y(s_i, t_j))$ ,  $t_j = -\pi + \pi(j-1)/N$ ,  $j = 1, \dots, 2N$ ,  $s_i = \pi(z_i + 1)/2$ ,  $i = 1, \dots, N$  with  $z_i \in (-1, 1)$  the  $N$ -point Gauss-Legendre quadrature rule abscissas with corresponding weights  $w_i$  for  $i = 1, \dots, N$ . One proceeds similarly for (21). We consider an exact solution of Problem (7):

$$u_{\text{exact}}(x) = \frac{1}{|x - x_0|}, \quad x_0 \in D,$$

which consists in choosing  $g(x^*) = \partial_{n_y} u_{\text{exact}}(x^*)$ , for any  $x^* \in \partial D$ . Figure 4 represents the error obtained using:

- **Method:** approximation of (8) using the three-step method.
- **DSL:** approximation of (21) using the the three-step method.

For all simulations we consider  $N = 16$ , and  $\partial D$  is a sphere of radius 2. We solve (9) using a Galerkin method and the product Gaussian quadrature rule [5, 6, 7, 8, 9] (see Appendix B for details), and the accuracy of both methods is limited by the accuracy of the resolution for  $\rho$ . Results in Figure-4 show that, given  $\rho$  resolved, the approximation of the modified representation provides better results overall. Note that the single-layer potential commonly suffers less from the close evaluation than the double-layer potential, and the chosen method provides already a good approximation. The modified representation allows to make it even better.

**Remark 2.** For simplicity results in three dimensions are computed on a sphere, where the resolution of  $\rho$  does not require a lot of quadrature points. One can apply the technique for arbitrary closed smooth surfaces, but might be limited by the resolution of (9).

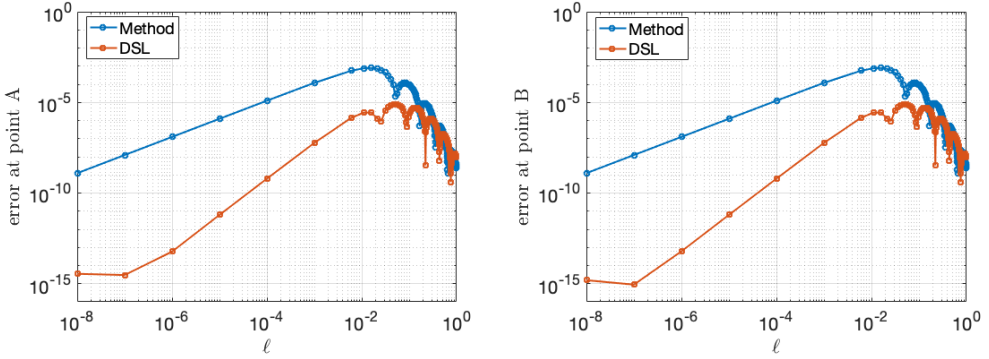


Figure 4 – Log-log plots of the errors made in computing the solution of (7) for the Neumann data,  $g(x^*) = -\frac{n_y \cdot (x^* - x_0)}{|x^* - x_0|^3}$  with  $x_0 = (0, 0, 0)$ , outside of a sphere a radius 2 using Method and DSL, along the normal of two points on the sphere: point A=(-0.0065,-0.0327,1.9997) (left), at the point B=(-0.3526,-1.7728,0.8561) (right).

## 5.2 Scattering problem

Using Proposition 2, we compare (11) with the modified representation (20) obtained with  $u_{\text{sol}}^H(y) = e^{ikn_{x^*} \cdot (y - x^*)}$ :

$$\begin{aligned} u(x) = & \int_{\partial D} \left[ \partial_{n_y} G(x, y) - ik(n_y \cdot n_{x^*}) e^{ik(n_{x^*} \cdot (y - x^*))} G(x, y) \right] [\mu(y) - \mu(x^*)] d\sigma_y \\ & + ik \int_{\partial D} [(n_y \cdot n_{x^*}) e^{ik(n_{x^*} \cdot (y - x^*))} - 1] G(x, y) \mu(y) d\sigma_y \\ & + \mu(x^*) \int_{\partial D} \partial_{n_y} G(x, y) [1 - e^{ik(n_{x^*} \cdot (y - x^*))}] d\sigma_y, \quad x \in \mathbb{R}^d \setminus \bar{D}. \end{aligned} \quad (24)$$

We'll refer to (24) as the modified representation using *Plane Wave Subtraction* technique (PWS).

### 5.2.1 Example 3: scattering in two dimensions

We consider an exact solution of Problem (10):

$$u_{\text{exact}}(x) = \frac{i}{4} H_0^{(1)}(k|x - x_0|), \quad x_0 \in D,$$

which consists in choosing  $f(x^*) = u_{\text{exact}}(x^*)$ , for any  $x^* \in \partial D$ . Figures 5-6 represent the error obtained on a star-shaped domain using:

- **PTR:** approximation of (11) using the Periodic Trapezoid Rule.
- **PWS:** approximation of (24) using the Periodic Trapezoid Rule.

In the simulations below we consider  $N = 256$  quadrature points, and  $k = 15$ . We solved (13) using Kress quadrature [30] (see Appendix A). The quadrature rule is well adapted to approximate kernels with a logarithmic singularity. The accuracy of both methods is

limited by the resolution for  $\mu$ . Results in Figures-5-6 show that, given  $\mu$  resolved, the approximation of the modified representation provides better results overall. Similarly to Laplace's examples, far from the boundary, both methods approximate well the solution. As the evaluation point gets closer to the boundary ( $\ell \rightarrow 0$ ), PTR suffers from the close evaluation problem leading to large errors. Using the modified representation (PWS) allows to reduce the error by a couple of order of magnitude for the close evaluation problem.

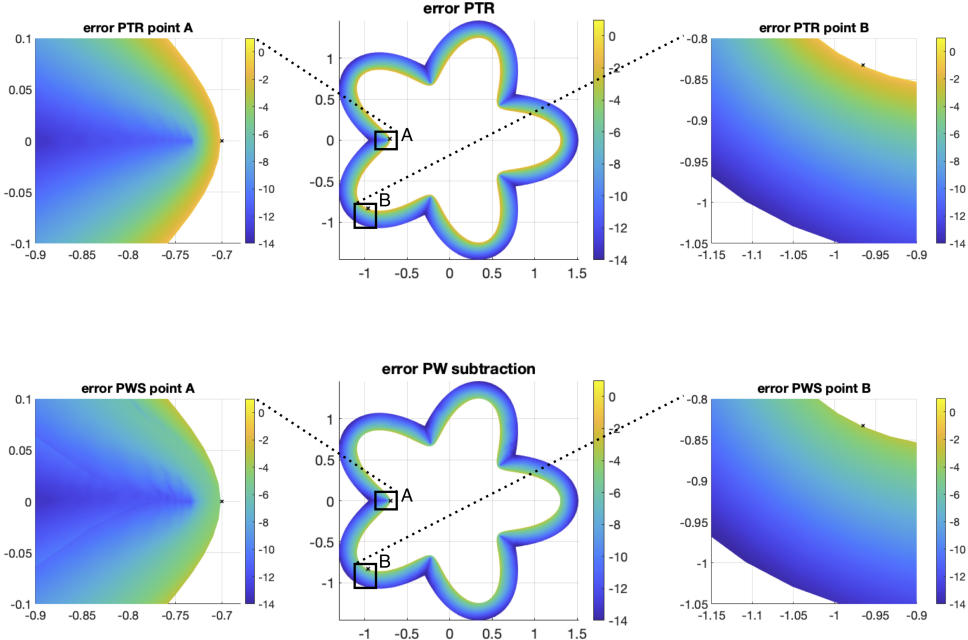


Figure 5 – Plots of  $\log_{10}$  of the error for the evaluation of the solution of (10) out of the star domain defined by the boundary  $y(t) = (1.55 + 0.4 \cos 5t) * (\cos t, \sin t)$ ,  $t \in [0, 2\pi]$ , for the Dirichlet data,  $f(x^*) = \frac{i}{4} H_0^{(1)}(15|x^* - x_0|)$  with  $x_0 = (0.2, 0.8)$ , using PTR (top), PWS (bottom), with  $N = 256$ .

### 5.2.2 Example 4: scattering in three dimensions

We consider an exact solution of (1):

$$u_{\text{exact}}(x) = \frac{1}{4\pi} \frac{e^{ik|x-x_0|}}{|x-x_0|}, \quad x_0 \in D,$$

which consists in choosing  $f(x^*) = u_{\text{exact}}(x^*)$ , for any  $x^* \in \partial D$ . Figure 7 represents the error obtained using:

- **Method:** approximation of (11) using the three-step method (see section 5.1.2).
- **PWS:** approximation of (24) using the three-step method.

For both simulations we consider  $N = 16$  quadrature points,  $k = 5$ , and  $\partial D$  is the sphere of radius 2 centered at the origin. We solved (13) using Galerkin method and the product

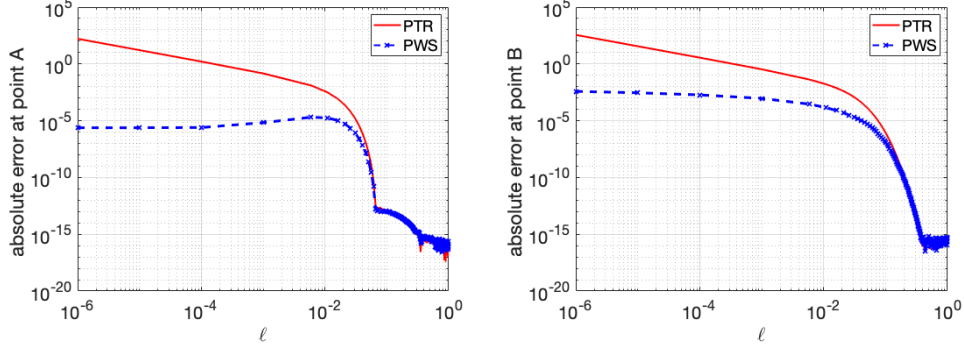


Figure 6 – Log-log plots of the errors made in computing the solution along the normal of the two points A, B, plotted as black  $\times$ ’s in Figure 5.

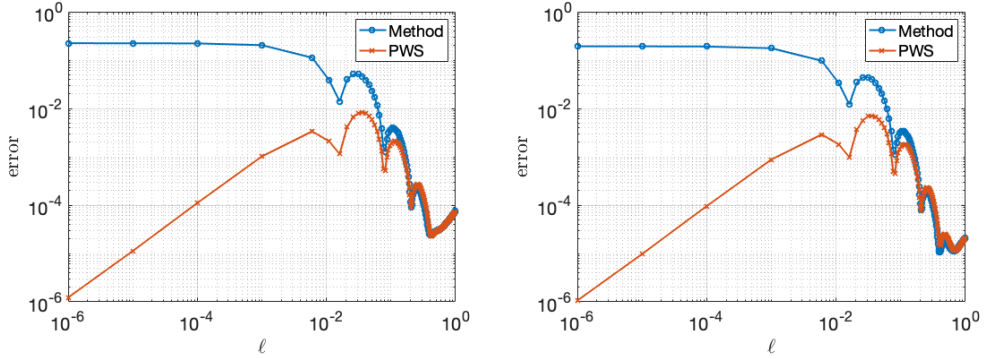


Figure 7 – Log-Log of the error along the normal for the evaluation of the solution of (10) out of sphere of radius 2 for the Dirichlet data,  $f(x^*) = \frac{1}{4} \frac{e^{i5|z-x_0|}}{|x-x_0|}$  with  $x_0 = (0.1, 0.2, 0.3)$ : at the point A=(-0.0065,-0.0327,1.9997) (left), at the point B=(-0.3526,-1.7728,0.8561) (right).

Gaussian quadrature rule (see Appendix B for details). The accuracy of both methods is limited by the accuracy of the resolution for  $\mu$ . Results in Figure-7 show that, given  $\mu$  resolved, standard representation incurs bigger errors at close evaluation points, while the modified representation provides much better results overall.

### 5.2.3 High frequency behavior

It is well-known that, for a fixed number of quadrature points  $N$ , accuracy is lost for larger wavenumbers  $k$ . Figure 8 represents the high frequency behavior for the Examples 3 and 4. We consider the same quadrature rules, number of quadrature points  $N$ , exact solution  $u_{\text{exact}}$ , boundary shapes, as in sections 5.2.1, 5.2.2, and we vary  $k$ . The modified representation annihilates some oscillatory behavior by subtracting plane waves along the normal of the evaluation points. It allows then a better approximation for a wider range of wavenumbers (until the number of quadrature points isn’t enough), and results

in a greater wavenumber stability. Results in Figure 8 confirm this phenomenon.

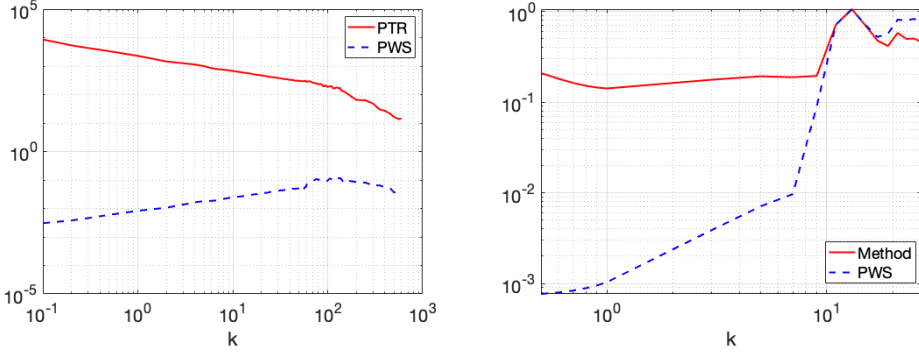


Figure 8 – Log-Log of the maximum error in computing the solution of Problem (10) as described in sections 5.2.1, 5.2.2, with respect to the wavenumber  $k$ : in 2D (left), in 3D (right).

## 6 Modified boundary integral equations

We have used Theorem 1 to modify the representation of solution of boundary value problems close to (but not on) the boundary. Theorem 1 also offers identities on the boundary, which could be used to avoid singular integrals in the boundary integral equation. In the section we present a modified representation of (13).

**Proposition 3.** *Given  $x^* \in \partial D$ , let  $u_{sol}^H$  be a solution of Helmholtz equation in  $D \subset \mathbb{R}^d$ ,  $d = 2, 3$ , satisfying conditions (19). Then the boundary integral equation (13) admits the modified representation:*

$$\begin{aligned} & \int_{\partial D} [\partial_{n_y} G^H(x^*, y) - \partial_{n_y} u_{sol}^H(y) G^H(x^*, y)] [\mu(y) - \mu(x^*)] d\sigma_y \\ & + \int_{\partial D} G^H(x^*, y) [\partial_{n_y} u_{sol}^H(y) - ik] \mu(y) d\sigma_y \\ & + \mu(x^*) \int_{\partial D} \partial_{n_y} G^H(x^*, y) [1 - u_{sol}^H(y)] d\sigma_y = f(x^*). \end{aligned} \quad (25)$$

The modified representation (25) has no singular integrals.

The proof can be found in Appendix C.3. Using again  $u_{sol}^H(y) = e^{ikn_{x^*} \cdot (y-x^*)}$ , Proposition 3 gives us the modified boundary integral equation:

$$\begin{aligned} & \int_{\partial D} [\partial_{n_y} G^H(x^*, y) - ik(n_y \cdot n_{x^*}) e^{ikn_{x^*} \cdot (y-x^*)} G^H(x^*, y)] [\mu(y) - \mu(x^*)] d\sigma_y \\ & + ik \int_{\partial D} G^H(x^*, y) [(n_y \cdot n_{x^*}) e^{ikn_{x^*} \cdot (y-x^*)} - 1] \mu(y) d\sigma_y \\ & + \mu(x^*) \int_{\partial D} \partial_{n_y} G^H(x^*, y) [1 - e^{ikn_{x^*} \cdot (y-x^*)}] d\sigma_y = f(x^*). \end{aligned} \quad (26)$$

Equation (26) has no singular integrals, in particular it could be approximated using standard quadrature rules such as PTR in two dimensions. We will refer to (26) as the boundary integral equation with plane wave subtraction (BIE-PWS). Going back to Examples 3 and 4 presented in sections 5.2.1, 5.2.2, we now compare the approximation PWS of (24), where the density  $\mu$  has been computed using the following methods:

- **BIE-Method:** approximation of (13) using Kress quadrature (2D), using product Gaussian quadrature rule (3D).
- **BIE-PWS:** approximation of (26) using PTR (2D), using product Gaussian quadrature rule (3D).

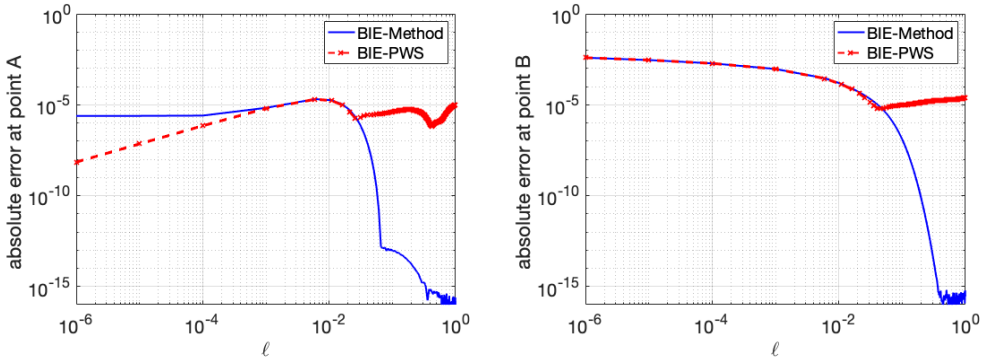


Figure 9 – Log-Log plot of the error along the normal for the solution of (10) out of the star domain defined by the boundary  $y(t) = (1.55 + 0.4 \cos 5t) * (\cos t, \sin t)$ ,  $t \in [0, 2\pi]$ , for the Dirichlet data,  $f(x^*) = \frac{i}{4} H_0^{(1)}(15|x^* - x_0|)$  with  $x_0 = (0.2, 0.8)$ , at the two points A,B, plotted as black  $\times$ 's in Figure 5.

Figure 9 represents the results in two dimensions and illustrates how the resolution of  $\mu$  limits the approximation of the solution of (10). Far from the boundary the error made using BIE-PWS cannot be better than order  $10^{-6}$ . This limitation is due to the poor resolution of  $\mu$  using BIE-PWS. However, as the evaluation point gets closer to the boundary ( $\ell \rightarrow 0$ ), BIE-PWS yields competitive, and sometimes better, results. The modified boundary integral equation (26) can be approximated using standard quadrature rules such as Periodic Trapezoid Rule (note that PTR was not possible to use to solve for (13) due to singular integrals). Its resolution may be limited but it offers interesting corrections for the close evaluation problem using simple quadrature rules.

Results in Figure 10 show that, in three dimensions, the resolution of the solution using both methods yields the same accuracy. The product Gaussian quadrature rule is an open quadrature at the singular point  $y = x^*$  (see Appendix B), therefore the modification introduced in (24) doesn't affect the approximation. The product Gaussian quadrature rule is a well-used, efficient, easy to implement method, but one could consider a closed quadrature rule to study the effect of (26) more closely.

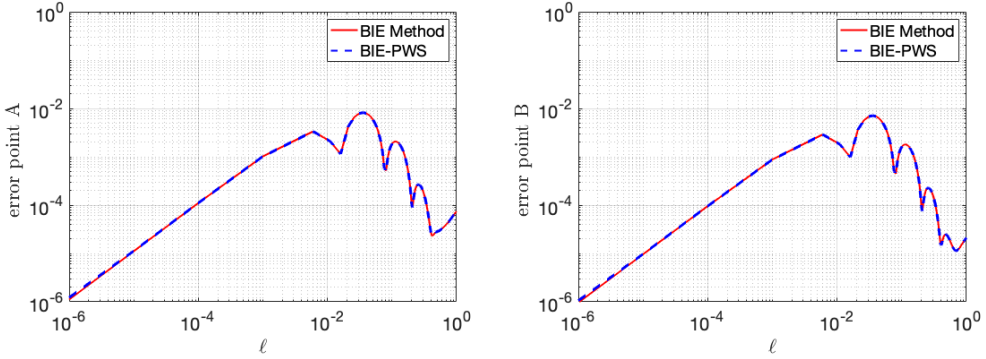


Figure 10 – Log-Log plot of the error along the normal of the solution of (10) out of the sphere of radius 2 for the Dirichlet data,  $f(x^*) = \frac{1}{4} \frac{e^{i5|z-x_0|}}{|x-x_0|}$  with  $x_0 = (0.1, 0.2, 0.3)$  with  $N = 16$ : at the point A=(-0.0065,-0.0327,1.9997) (left), at the point B=(-0.3526,-1.7728,0.8561) (right).

## 7 Conclusion

In this paper we have established new identities for Laplace and Helmholtz layer potentials, and used them to address the close evaluation problem in several boundary value problems. Similar to Gauss' law, these identities take advantage of solutions of the partial differential equation at stake. These identities can also be used to modify the boundary integral equation to avoid weakly singular integrals. Several examples in two and three dimensions have been presented and demonstrated the efficiency of the modified representation. Given a quadrature rule, the modified representation of the solution provides a better approximation by several orders of magnitude. This assumes that the density, solution of the boundary integral equation, is well-resolved. The modified boundary integral equation has no singular behaviors anymore, and allows us to use standard quadrature rules that do not treat singularities.

One can use these identities to modify any other wave problems, including sound-hard, penetrable obstacles. Future work includes applying those techniques to plasmonic scattering problems [24, 4], deriving an asymptotic analysis to quantify the limit behavior of the error as the evaluation point approaches the boundary, as well as extensions to other partial differential equations such as Stokes problems and others.

## A Kress quadrature

In this section we provide a brief summary about the Kress quadrature [30] used to compute the density  $\mu$ , solution of (13), in two dimensions. Denoting  $y(t)$ ,  $t \in (0, 2\pi)$  the parameterization of  $\partial D$ , and denoting  $x^* = y(t^*)$ , we compactly rewrite (13)

$$\frac{1}{2}\mu(t^*) + \int_0^{2\pi} K(t, t^*)\mu(t) dt = f(t^*), \quad (27)$$

with the abuse of notation  $K(t, t^*) = (\partial_{n_y} G(x^*, y(t)) - ikG(x^*, y(t))) |y'(t)|$ ,  $\mu(t) = \mu(y(t))$ , and  $f(t) = f(y(t))$ . Kress quadrature is well adapted for weakly singular integrals involving kernel with a logarithmic singularity. To that aim one rewrites:

$$K(t, t^*) = K_1(t, t^*) \log \left( 4 \sin^2 \left( \frac{t^* - t}{2} \right) \right) + K_2(t, t^*),$$

with smooth functions  $K_1, K_2$  (the expression of  $K_1, K_2$  can be found in [30]). Then one discretizes the integral as follows:

$$\int_0^{2\pi} K(t, t^*) \mu(t) dt \approx \sum_{k=0}^N \left( R_k^{(n)}(t^*) K_1(t^*, t_k) + \frac{2\pi}{N} K_2(t^*, t_k) \right) \mu(t_k),$$

with  $t_k = \frac{2\pi k}{N}$ ,  $k = 0, \dots, N$ , and  $R_k^{(n)}(t^*)$  the weights

$$R_k^{(n)}(t^*) = -\frac{4\pi}{N} \sum_{j=1}^{N/2} \frac{1}{j} \cos(j(t^* - t_k)) - \frac{4\pi}{N^2} \cos \left( \frac{N}{2}(t^* - t_k) \right), \quad k = 0, \dots, N.$$

## B Galerkin approximation

In this section we provide a brief summary about the Galerkin approximation used to compute the solutions of (4)-(9)-(13)-(26) in three dimensions. First, we compactly write (4)-(9)-(13)-(26) as

$$\mathcal{K}[\psi] = F, \quad (28)$$

with  $\psi$  denoting the density (i.e.  $\mu, \rho$ ), and  $F$  denoting the Dirichlet or Neumann data. We introduce the approximation for  $\psi$ ,

$$\psi(y(\theta, \varphi)) \approx \sum_{n=0}^{N-1} \sum_{m=-n}^n Y_{nm}(\theta, \varphi) \hat{\psi}_{nm}, \quad (29)$$

with  $y(\theta, \varphi)$ ,  $\theta \in (0, \pi)$ ,  $\varphi \in (-\pi, \pi)$  a parameterization of the boundary  $\partial D$ ,  $\{Y_{nm}(\theta, \varphi)\}_{n,m}$  the orthonormal set of spherical harmonics. For  $x^* \in \partial D$ , we write  $x^* = y(\theta^*, \varphi^*)$ . Note that  $N$  in (29) corresponds also to the same order of the quadrature rule used to approximate (4)-(9)-(13)-(26). Substituting (29) into (28) and taking the inner product with  $Y_{n'm'}(\theta^*, \varphi^*)$ , we obtain the Galerkin equations,

$$\sum_{n=0}^{N-1} \sum_{m=-n}^n \langle Y_{n'm'}, \mathcal{K}[Y_{nm}] \rangle \hat{\psi}_{nm} = \langle Y_{n'm'}, F \rangle. \quad (30)$$

We construct the  $N^2 \times N^2$  linear system for the unknown coefficients,  $\hat{\psi}_{n'm'}$  resulting from (30) evaluated for  $n' = 0, \dots, N-1$  with corresponding values of  $m'$ . To compute the inner products,  $\langle Y_{n'm'}, \mathcal{K}[Y_{nm}] \rangle$  and  $\langle Y_{n'm'}, F \rangle$ , we use the product Gaussian quadrature rule for spherical integrals [5]. This corresponds to approximate the integral with

respect to  $\varphi$  using  $N$  Gauss-Legendre quadrature points, and the integral with respect to  $\theta$  using a  $2N$  Periodic Trapezoid Rule points. One can proceed as in the three-step method (see section 5.1.2, and [27] for more details), by adding a rotation of the local coordinate system so that  $x^*$  corresponds to the north pole, and by using the  $N$  Gauss-Legendre quadrature points mapped to  $(0, \pi)$  and not  $(-1, 1)$ .

For (4), we have

$$\begin{aligned}\mathcal{K}[Y_{nm}](\theta^*, \varphi^*) &= -\frac{1}{2}Y_{nm}(\theta^*, \varphi^*) \\ &\quad + \int_{-\pi}^{\pi} \int_0^{\pi} \partial_{n_y} G^L(\theta^*, \varphi^*, \theta, \varphi) J(\theta, \varphi) \sin(\theta) Y_{nm}(\theta, \varphi) d\theta d\varphi.\end{aligned}$$

For (9), we make use of the adjoint  $\mathcal{K}^*$  of  $\mathcal{K}$ . Using (5) we write  $\sum_{n=0}^{N-1} \sum_{m=-n}^n \langle \mathcal{K}^*[Y_{n'm'}], Y_{nm} \rangle \hat{\psi}_{nm} = \langle Y_{n'm'}, F \rangle$ . with

$$\begin{aligned}\mathcal{K}^*[Y_{n'm'}](\theta, \varphi) &= \int_{-\pi}^{\pi} \int_0^{\pi} \partial_{n_x^*} G^L(\theta^*, \varphi^*, \theta, \varphi) J(\theta^*, \varphi^*) \sin(\theta^*) \\ &\quad [Y_{n'm'}(\theta^*, \varphi^*) - Y_{n'm'}(\theta, \varphi)] d\theta^* d\varphi^*.\end{aligned}$$

For (13), we have

$$\begin{aligned}\mathcal{K}[Y_{nm}](\theta^*, \varphi^*) &= \frac{1}{2}Y_{nm}(\theta^*, \varphi^*) + \int_{-\pi}^{\pi} \int_0^{\pi} [\partial_{n_y} G^H(\theta^*, \varphi^*, \theta, \varphi) - ik G^H(\theta^*, \varphi^*, \theta, \varphi)] \\ &\quad J(\theta, \varphi) \sin(\theta) Y_{nm}(\theta, \varphi) d\theta d\varphi,\end{aligned}$$

and for (26) we have

$$\begin{aligned}\mathcal{K}_m[Y_{nm}](\theta^*, \varphi^*) &= \\ &\int_{-\pi}^{\pi} \int_0^{\pi} [\partial_{n_y} G^H(\theta^*, \varphi^*, \theta, \varphi) - ik(n_y \cdot n_{x^*}) e^{ik(n_{x^*} \cdot (y(\theta, \varphi) - y(\theta^*, \varphi^*))}] G^H(\theta^*, \varphi^*, \theta, \varphi) \\ &\quad J(\theta, \varphi) \sin(\theta) [Y_{nm}(\theta, \varphi) - Y_{nm}(\theta^*, \varphi^*)] d\theta d\varphi \\ &+ ik \int_{-\pi}^{\pi} \int_0^{\pi} [(n_y \cdot n_{x^*}) e^{ik(n_{x^*} \cdot (y(\theta, \varphi) - y(\theta^*, \varphi^*))} - 1] G^H(\theta^*, \varphi^*, \theta, \varphi) J(\theta, \varphi) \sin(\theta) Y_{nm}(\theta, \varphi) d\theta d\varphi \\ &+ Y_{nm}(\theta^*, \varphi^*) \int_{-\pi}^{\pi} \int_0^{\pi} [1 - e^{ik(n_{x^*} \cdot (y(\theta, \varphi) - y(\theta^*, \varphi^*))}] \partial_{n_y} G^H(\theta^*, \varphi^*, \theta, \varphi) J(\theta, \varphi) \sin(\theta) d\theta d\varphi.\end{aligned}$$

## C Proof of modified representations

### C.1 Modified double-layer potential 15

Given  $u_{\text{sol}}^L$  solution of Laplace's equation in  $D \subset \mathbb{R}^d$ ,  $d = 2, 3$ , and for  $x \in D$  we write  $x = x^* - \ell n_{x^*}$ , with  $x^* \in \partial D$ . Then we write (2) as:

$$\begin{aligned} u(x) &= \int_{\partial D} \partial_{n_y} G^L(x, y) \mu(y) [1 - u_{\text{sol}}^L(y)] d\sigma_y + \int_{\partial D} \partial_{n_y} G^L(x, y) \mu(y) u_{\text{sol}}^L(y) d\sigma_y \\ &= \int_{\partial D} \partial_{n_y} G^L(x, y) \mu(y) [1 - u_{\text{sol}}^L(y)] d\sigma_y + \int_{\partial D} \partial_{n_y} G^L(x, y) [\mu(y) - \mu(x^*)] u_{\text{sol}}^L(y) d\sigma_y \\ &\quad + \mu(x^*) \int_{\partial D} \partial_{n_y} G^L(x, y) u_{\text{sol}}^L(y) - G^L(x, y) \partial_{n_y} u_{\text{sol}}^L(y) d\sigma_y + \mu(x^*) \int_{\partial D} G^L(x, y) \partial_{n_y} u_{\text{sol}}^L(y) d\sigma_y \end{aligned}$$

Using Theorem 1, the third term becomes  $-\mu(x^*) u_{\text{sol}}^L(x^*)$ , then

$$\begin{aligned} u(x) &= \int_{\partial D} \partial_{n_y} G^L(x, y) \mu(y) [1 - u_{\text{sol}}^L(y)] d\sigma_y + \int_{\partial D} \partial_{n_y} G^L(x, y) [\mu(y) - \mu(x^*)] u_{\text{sol}}^L(y) d\sigma_y \\ &\quad - \mu(x^*) u_{\text{sol}}^L(x^*) + \mu(x^*) \int_{\partial D} G^L(x, y) [\partial_{n_y} u_{\text{sol}}^L(y) - \partial_{n_y} u_{\text{sol}}^L(x^*)] d\sigma_y \\ &\quad + \mu(x^*) \partial_{n_y} u_{\text{sol}}^L(x^*) \int_{\partial D} G^L(x, y) d\sigma_y \end{aligned}$$

which is (15).

### C.2 Proof of Proposition 1

In this section we derive (18). Given  $u_{\text{sol}}^L$  solution of Laplace's equation in  $D \subset \mathbb{R}^d$ ,  $d = 2, 3$ , and for  $x \in E$  we write  $x = x^* + \ell n_{x^*}$ , with  $x^* \in \partial D$ . Then we write (8) as:

$$\begin{aligned} u(x) &= \int_{\partial D} G^L(x, y) \mu(y) [1 - \partial_{n_y} u_{\text{sol}}^L(y)] d\sigma_y + \int_{\partial D} G^L(x, y) \mu(y) \partial_{n_y} u_{\text{sol}}^L(y) d\sigma_y \\ &= \int_{\partial D} G^L(x, y) \mu(y) [1 - \partial_{n_y} u_{\text{sol}}^L(y)] d\sigma_y + \int_{\partial D} G^L(x, y) [\mu(y) - \mu(x^*)] \partial_{n_y} u_{\text{sol}}^L(y) d\sigma_y \\ &\quad + \mu(x^*) \int_{\partial D} G^L(x, y) \partial_{n_y} u_{\text{sol}}^L(y) - \partial_{n_y} G^L(x, y) u_{\text{sol}}^L(y) d\sigma_y \\ &\quad + \mu(x^*) \int_{\partial D} \partial_{n_y} G^L(x, y) u_{\text{sol}}^L(y) d\sigma_y \end{aligned}$$

Using Theorem 1, the third term vanishes, then

$$\begin{aligned} u(x) &= \int_{\partial D} \partial_{n_y} G^L(x, y) \mu(y) [1 - u_{\text{sol}}^L(y)] d\sigma_y + \int_{\partial D} \partial_{n_y} G^L(x, y) [\mu(y) - \mu(x^*)] u_{\text{sol}}^L(y) d\sigma_y \\ &\quad + \mu(x^*) \int_{\partial D} \partial_{n_y} G^L(x, y) [u_{\text{sol}}^L(y) - u_{\text{sol}}^L(x^*)] d\sigma_y + \mu(x^*) u_{\text{sol}}^L(x^*) \int_{\partial D} \partial_{n_y} G^L(x, y) d\sigma_y \end{aligned}$$

The last term vanishes using Gauss' law (5), then one obtains (18).

### C.3 Proof of Propositions 2, 3

In this section we derive (20), (25). Given  $u_{\text{sol}}^H$  solution of the Helmholtz equation in  $D \subset \mathbb{R}^d$ ,  $d = 2, 3$ , and for  $x \in E$  we write  $x = x^* + \ell n_{x^*}$ , with  $x^* \in \partial D$ . Then we write (11) as:

$$\begin{aligned}
u(x) &= \int_{\partial D} [\partial_{n_y} G^H(x, y) - \partial_{n_y} u_{\text{sol}}^H(y) G^H(x, y)] \mu(y) d\sigma_y \\
&\quad + \int_{\partial D} [\partial_{n_y} u_{\text{sol}}^H(y) - ik] G^H(x, y) \mu(y) d\sigma_y \\
&= \int_{\partial D} [\partial_{n_y} G^H(x, y) - \partial_{n_y} u_{\text{sol}}^H(y) G^H(x, y)] [\mu(y) - \mu(x^*)] d\sigma_y \\
&\quad + \int_{\partial D} [\partial_{n_y} u_{\text{sol}}^H(y) - ik] G^H(x, y) \mu(y) d\sigma_y \\
&\quad + \mu(x^*) \int_{\partial D} [\partial_{n_y} G^H(x, y) u_{\text{sol}}^H(y) - \partial_{n_y} u_{\text{sol}}^H(y) G^H(x, y)] d\sigma_y \\
&\quad + \mu(x^*) \int_{\partial D} \partial_{n_y} G^H(x, y) [(1 - u_{\text{sol}}^H(y))] d\sigma_y
\end{aligned} \tag{31}$$

Using Theorem 1, the third term vanishes, then one obtains (20). One proceeds similarly starting with (13), one can show that the layer potentials in (13) correspond to (31) for  $x = x^* \in \partial D$ . Theorem 1 gives that the third term boils down to  $-\frac{1}{2}\mu(x^*)u_{\text{sol}}^H(x^*)$ , which finishes the proof.

**Acknowledgements.** This research was supported by National Science Foundation Grant: DMS-1819052. The author would like to thank S. Khatri, A. D. Kim, and Z. Moitier for fruitful discussions.

## References

- [1] af Klinteberg L., Tornberg A.-K., A fast integral equation method for solid particles in viscous flow using quadrature by expansion, *J. Comput. Phys.* 326 (2016) 420–445.
- [2] af Klinteberg L., Tornberg A.-K., Error estimation for quadrature by expansion in layer potential evaluation, *Adv. Comput. Math.* 43 (1) (2017) 195–234.
- [3] Akselrod G. M., Argyropoulos C., Hoang T. B., Ciraci C., Fang C., Huang J., Smith D. R., Mikkelsen M. H., Probing the mechanisms of large Purcell enhancement in plasmonic nanoantennas, *Nat. Photonics* 8 (2014) 835–840.
- [4] Ammari H., Millien P., Ruiz M., Zhang H., Mathematical analysis of plasmonic nanoparticles: the scalar case., *Archive for Rational Mechanics and Analysis*, 2 (2017) 597–658.
- [5] Atkinson K. E., Numerical integration on the sphere, *ANZIAM J.* 23 (3) (1982) 332–347.

- [6] Atkinson K. E., The numerical solution Laplace's equation in three dimensions, SIAM J. Numer. Anal. 19 (2) (1982) 263–274.
- [7] Atkinson K. E., Algorithm 629: An integral equation program for Laplace's equation in three dimensions, ACM Trans. Math. Softw. 11 (2) (1985) 85–96.
- [8] Atkinson K. E., A survey of boundary integral equation methods for the numerical solution of Laplace's equation in three dimensions, in: Numerical Solution of Integral Equations, Springer (1990) 1–34.
- [9] Atkinson K. E., The Numerical Solution of Integral Equations of the Second Kind, Cambridge University Press, 1997.
- [10] Barnett A. H., Evaluation of layer potentials close to the boundary for Laplace and Helmholtz problems on analytic planar domains, SIAM J. Sci. Comput. 36 (2) (2014) A427–A451.
- [11] Barnett A. H., Wu B., Veerapaneni S., Spectrally accurate quadratures for evaluation of layer potentials close to the boundary for the 2D Stokes and Laplace equations, SIAM J. Sci. Comp. 37 (2015) B519–B542.
- [12] Beale J. T., Lai M. C., A method for computing nearly singular integrals, SIAM J. Numer. Anal. 38 (6) (2001) 1902–1925.
- [13] J. T. Beale, W. Ying, J. R. Wilson, A simple method for computing singular or nearly singular integrals on closed surfaces, Commun. Comput. Phys. 20 (3) (2016) 733–753.
- [14] Bremer J., Gimbutas Z., Rokhlin V., A nonlinear optimization procedure for generalized gaussian quadratures, SIAM J. Sci. Comp. 32 (4) (2010) 1761–1788.
- [15] Bruno O. P., Kunyansky L. A., A fast, high-order algorithm for the solution of surface scattering problems: basic implementation, tests, and applications, J. Comput. Phys. 169 (1) (2001) 80–110.
- [16] Cakoni F., Colton, C. *Qualitative methods in inverse scattering theory. An introduction*, Springer-Verlag, Interaction of Mechanics and Mathematics, Berlin, 2006.
- [17] Carvalho C., Subtraction-techniques codes, 2020 <https://doi.org/10.5281/zenodo.3934284>.
- [18] Carvalho C., Khatri S., Kim A. D., Asymptotic analysis for close evaluation of layer potentials, J. Comput. Phys. 355 (2018) 327–341.
- [19] Carvalho C., Khatri S., Kim A. D., Asymptotic approximation for the close evaluation of double-layer potentials, SIAM J. Sci. Comp. 42 (1) (2020) A504–A533.
- [20] Colton D., Kress R., *Integral equation methods in scattering theory*, SIAM, 2013.
- [21] Epstein C. L., Greengard L., Klöckner A. K., On the convergence of local expansions of layer potentials, SIAM J. Numer. Anal. 51 (5) (2013) 2660–2679.
- [22] Ganesh M., Graham I., A high-order algorithm for obstacle scattering in three dimensions, Journal of Computational Physics 198 (1) (2004) 211–242.
- [23] Guenther R. B., Lee J. W., Partial Differential Equations of Mathematical Physics and Integral Equations, Dover Publications, 1996.

- [24] Helsing J., Karlsson A., An extended charge-current formulation of the electromagnetic transmission problem, SIAM J. App. Math. 80 (2020) 951–976.
- [25] Helsing J., Ojala, R. On the evaluation of layer potentials close to their sources, J. Comput. Phys. 227 (5) (2008) 2899–2921.
- [26] Keaveny E. E., Shelley M. J., Applying a second-kind boundary integral equation for surface tractions in Stokes flow, J. Comput. Phys. 230 (2011) 2141–2159.
- [27] Khatri S., Kim A. D., Cortes R., Carvalho C., Close evaluation of layer potentials in three dimensions, in revision. arXiv: 1807.02474, 2019.
- [28] Klöckner A., Barnett A., Greengard L., O’Neil M., Quadrature by expansion: A new method for the evaluation of layer potentials, J. Comput. Phys. 252 (2013) 332–349.
- [29] Kress R., *Linear Integral Equations*, Springer, 1989.
- [30] Kress R., Boundary integral equations in time-harmonic acoustic scattering, Math. Comp. Mod. 15 (1991) 229–243.
- [31] Marple G. R., Barnett A., Gillman A., Veerapaneni S., A fast algorithm for simulating multiphase flows through periodic geometries of arbitrary shape, SIAM J. Sci. Comput. 38 (2016) B740–B772.
- [32] Mayer K. M., Lee S., Liao H., Rostro B. C., Fuentes A., Scully P. T., Nehl C. L., Hafner J. H., A label-free immunoassay based upon localized surface plasmon resonance of gold nanorods, ACS Nano 2 (2008) 687–692.
- [33] Novotny L., Van Hulst N., Antennas for light, Nat. Photonics 5 (2011) 83–90.
- [34] Pérez-Arancibia C., A plane-wave singularity subtraction technique for the classical Dirichlet and Neumann combined field integral equations, Appl. Numer. Math. 123 (2018) 221–240.
- [35] Pérez-Arancibia C., Faria L., Turc, C. Harmonic density interpolation methods for high-order evaluation of Laplace layer potentials in 2D and 3D, J. Comput. Phys. 376 (2019) 411–434.
- [36] Pérez-Arancibia C., Turc C., Faria L., Planewave density interpolation methods for 3D Helmholtz boundary integral equations, SIAM J. Sci. Comp. 41 (4) (2019) A2088–A2116.
- [37] Rachh M., Klöckner A., O’Neil M., Fast algorithms for quadrature by expansion i: Globally valid expansions, J. Comput. Phys. 345 (2017) 706–731.
- [38] Sannomiya T., Hafner C., Voros J., In situ sensing of single binding events by localized surface plasmon resonance, Nano Lett. 8 (2008) 3450–3455.
- [39] Schwab C., Wendland W., On the extraction technique in boundary integral equations, Math. Comput. 68 (225) (1999) 91–122.
- [40] Smith D. J., A boundary element regularized Stokeslet method applied to cilia-and flagella-driven flow, Proc. R. Soc. Lond. A 465 (2009) 3605–3626.
- [41] Wala M., Klöckner A., A fast algorithm for Quadrature by Expansion in three dimensions, J. Comput. Phys. 388 (2019) 655–689.